PHYSICAL REVIEW E, VOLUME 65, 060701(R)

Effect of director distortions on morphologies of phase separation in liquid crystals

D. Voloschenko, O. P. Pishnyak, S. V. Shiyanovskii, and O. D. Lavrentovich
Chemical Physics Interdisciplinary Program and Liquid Crystal Institute, Kent State University, Kent, Ohio 44242
(Received 18 June 2001; published 10 June 2002)

We study phase separation from a nematic liquid crystal with spatially nonuniform director gradients. Particles of a phase-separated component, which is either an isotropic fluid (silicone oil) or a nonmesogenic photopolymer, accumulate in the regions with the strongest director distortions, thus reducing the overall energy of the system.

DOI: 10.1103/PhysRevE.65.060701 PACS number(s): 61.30.Gd, 64.75.+g

Phase separation (PS) in liquid crystals (LCs) is a subject of intensive studies [1–13]. A popular method to produce composites such as polymer-dispersed LCs (PDLCs) and polymer-stabilized LCs (PSLCs) is photoinduced PS in a mixture of a non-reactive LC and a reactive monomer. PS morphology depends on solubility [2], diffusivity [3], concentration [4], and reactivity of components, spatial distribution of light intensity [5], electric field gradients [6], time scales of reactions [7–9], and, importantly, on the orientational order of the LC solvent. For example, phase-separating droplets of silicone oil in a uniform LC gather in chains parallel to the director $\hat{\mathbf{n}}$ [10]. In PSLCs formed from a mesogenic monomer, polymer strands can align along $\hat{\mathbf{n}}$ [1,11]. An interesting problem is how the morphology would be altered if $\hat{\mathbf{n}}$ is distorted nonuniformly in space. Experiments on cholesteric gratings demonstrate that the precipitating component has a density modulation with the period set by the modulated $\hat{\mathbf{n}}$ [12,13], but the possible mechanisms are difficult to separate. In this work we use two different systems to demonstrate that spatial variation of the director gradients can lock-in the spatial distribution of the phase-separated component.

Temperature-induced PS. We use the nematic E7 (Merck) doped with 2 wt % of ''silicone oil'' poly(dimethylsiloxane-co-methylphenylsiloxane) (Aldrich 37,848-8), aligned in thin ($d=20\ \mu$m) cells by a rubbed polyvinyl alcohol. The system is the same as in Ref. [10], but the rubbing directions at the plates are perpendicular to each other (twisted nematic cell). The equally probable domains of left and right $\pi/2$ twists are separated by defects with strong director gradients [14]. PS was caused by a rapid (30 °C/min) quench from 55 °C (homogeneous nematic) to 15 °C.

PS starts at 48 °C [10]. The isotropic silicone oil-enriched particles appear everywhere, within the twist domains and at the domain boundaries. However, many particles migrate from within the domains toward the boundaries and accumulate there, see Fig. 1.

Polymerization-induced PS. We use E7 with 5 wt % of the UV-curable prepolymer NOA65 [15]. Photoinduced cross-linking results in compact morphologies; LC is expelled from the polymerized NOA65 which is often used as a matrix in PDLCs [6,8,9,16–19]. Because of a small concentration of NOA65, our system is a ''reverse'' of PDLCs. The noncured mixture preserves the nematic state up to 53 °C [16]. We used a narrow-band UV lamp (wavelength $\lambda=366$ nm) and a Glan-Thompson prism to polarize UV light linearly; impinging light intensity was $\approx 30\mu$W/cm^2. Experiments were performed at room temperature for cells with $d=20\ \mu$m.

There are three mechanisms of spatial nonuniformity in photoinduced PS. (a) Polymer density might vary because the angle between light polarization $\mathbf{P}$ and $\hat{\mathbf{n}}$ varies in space. (b) ''Lens'' effects in the distorted birefringent LC. (c) Because the LC is an elastic medium, the phase separating component might accumulate in the sites with the highest energy of director distortions, especially when this component forms compact particles rather than fibrils. We first show that the polymerization rate indeed depends on the angle between $\mathbf{P}$ and $\hat{\mathbf{n}}$.

(*a*) *Light polarization*. The cell plates were treated for uniform planar alignment (rubbed polyimide 2555, Microsystems), $\hat{\mathbf{n}}=$const. Photopolymerization was induced by UV light with $\mathbf{P}\perp\hat{\mathbf{n}}$ or $\mathbf{P}\parallel\hat{\mathbf{n}}$. Polymerization is faster when $\mathbf{P}\parallel\hat{\mathbf{n}}$, Fig. 2. The first hour of irradiation does not cure NOA65 completely: if irradiation is stopped and the sample is heated to 35–50 °C, the NOA65-rich particles dissolve back into the nematic matrix. Note also that the NOA65 particles often form chains along the groves of rubbed polyimide; patterned substrates can influence the PS morphologies [20].

(*b*) *Lens effect*. We return to twisted cells (rubbed polyimide), as they allow us to separate the lens and polarization

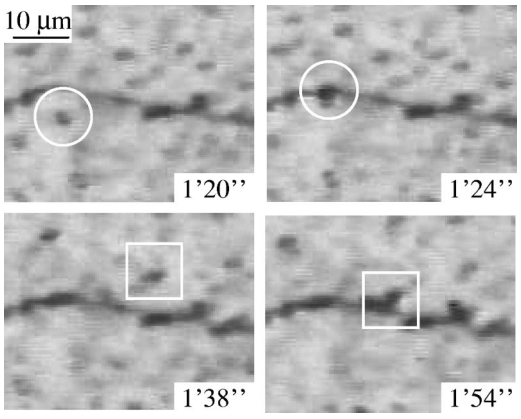

FIG. 1. PS dynamics in the E7/silicone oil mixture near the (horizontal) boundary separating two twist domains. Marked silicone oil particles migrate to the boundary from opposite directions.

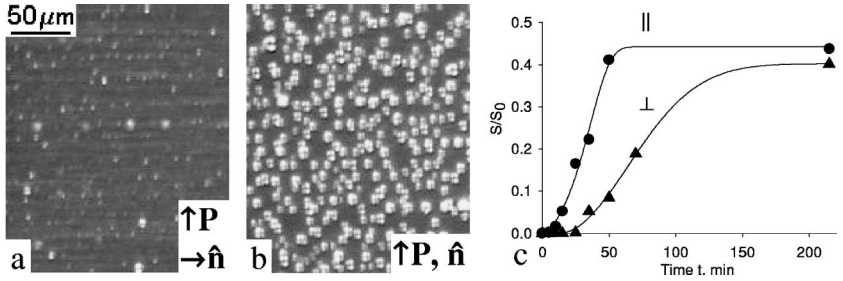

FIG. 2. Polymerization dynamics in a planar E7/NOA65 cell. Microphotographed after 35 min of UV exposure with (a) $\mathbf{P}\perp\hat{\mathbf{n}}$ and (b) $\mathbf{P}\|\hat{\mathbf{n}}$. Bright spots represent NOA65-rich particles. (c) S/S_0 vs irradiation time for $\mathbf{P}\perp\hat{\mathbf{n}}$ (triangles) and $\mathbf{P}\|\hat{\mathbf{n}}$ (circles); S is the area occupied by precipitated particles, as seen under the microscope; S_0 is the whole area of the charge-coupled device frame.

effects from the effect of distortions (c), by choosing $\mathbf{P}||\hat{\mathbf{n}}$ at the irradiated plate, Fig. 3. As $d \gg \lambda$, $\mathbf{P}$ rotates with $\hat{\mathbf{n}}$, remaining parallel to $\hat{\mathbf{n}}$ (Mauguin regime) within the twist domains. Therefore, the polarization effect facilitates polymerization within the twist domains but not at the domain boundary, where the Mauguin regime is violated [14] and $\mathbf{P}$ is not parallel to $\hat{\mathbf{n}}$. Furthermore, light with $\mathbf{P}\|\hat{\mathbf{n}}$ propagates with a refractive index n_e, which is the maximum value of the refractive index in the optically positive E7; thus if the domain boundary acts as a lens, this lens can be only divergent. Therefore, both polarization (a) and lens (b) effects facilitate NOA65 precipitation within the domains but not at their boundaries.

(c) *Director gradients*. As in the silicone oil PS, Fig. 1, the NOA65-rich particles appear everywhere, but many migrate toward the domain boundaries with strong distortions of $\hat{\mathbf{n}}$, Fig. 3. This effect in twisted cell is favored only by the mechanism (c). Smaller particles might coalesce into chains of big particles or even form continuous walls, Fig. 4.

Mechanism. Qualitatively, the leading mechanism causing phase-separated particles to aggregate in the regions with the highest LC distortions can be explained as follows. Initially, the nematic order is preserved in the whole specimen [21]. A phase-separated (oil or polymer) particle of radius R_p eliminates the nematic order in the volume $V_P \sim R_P^3$. The change in the free energy caused by placing a particle in a distorted LC is

$$\Delta E = -E_V + \Delta E_S + E_{ind}. \tag{1}$$

Here E_V is the elastic energy of the excluded volume V_P,

$$E_V \cong \frac{1}{2} K \int_{V_P} \frac{\partial n_i}{\partial x_j} \frac{\partial n_i}{\partial x_j} dV_P \cong \frac{2}{3} \pi K \frac{R_p^3}{\xi^2} A^2, \tag{2}$$

ΔE_S is the difference in the anchoring energy at the particle surface for homogeneous and distorted director fields, E_{ind} is the elastic energy of the additional distortions induced by the particle, K is the average Frank elastic constant, A is the amplitude, and ξ is the characteristic length of director distortions.

If $\hat{\mathbf{n}}$ were uniform, there would be no preferable site for the particle in the plane of the cell. However, in a distorted LC, elimination of the volume R_P^3 decreases the elastic energy by E_V. The stronger the distortions A/ξ, the higher the energy gain, Eq. (2). Similar consideration applies to particles covering a surface area with a large deviation of $\hat{\mathbf{n}}$ from the easy axis at the cell plates.

The importance of the two other terms in Eq. (1) depends on whether R_p is smaller or larger than the length $L_p = K/W_p$; W_p is the anchoring coefficient at the particle-nematic interface. Generally, $L_p \sim (0.1-10)$ μm; for the

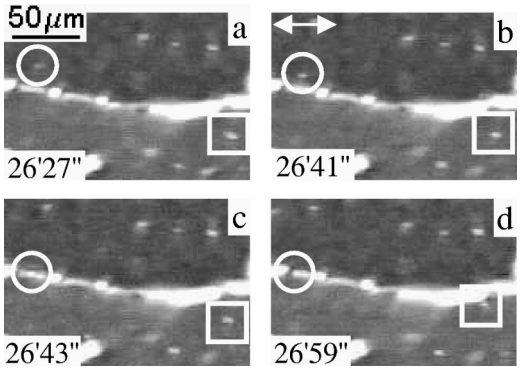

FIG. 3. UV photopolymerization near the (horizontal) defect boundary separating two twist domains in E7/NOA65. Marked NOA65 particles migrate to the boundary. The double arrow shows the directions of both $\mathbf{P}$ and $\hat{\mathbf{n}}$ at the cell plate facing the UV lamp. Time bars show the UV exposure time. Polarizing microscopy with uncrossed polarizers.

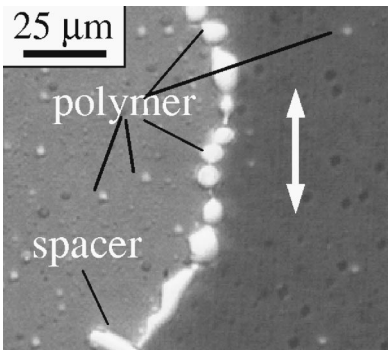

FIG. 4. Phase-separated E7/NOA65 near the defect boundary between two twist domains. UV exposure is 1 h. Uncrossed polarizers.

oil-E7 interface, $L_p \approx 2\ \mu$m [10]. When $R_p > L_p$, $\hat{\mathbf{n}}$ around the particle is determined mainly by the particle's surface properties; the gain E_V might be larger or smaller than the energy E_{ind} of additional distortions induced by the particle. There are cases when $E_V > E_{ind}$ undoubtedly. For example, a sphere with perpendicular anchoring placed in the LC with a radial $\hat{\mathbf{n}}$ (the hedgehog defect) finds the energy minimum at the defect core [22]. It is, however, hard to find a universal description of E_{ind} and E_V when $R_p > L_p$. Fortunately, it is the case $R_p < L_p$ that is of interest in PS. As demonstrated experimentally by Loudet *et al.* [10], the particle size is stabilized at $R_p \simeq L_p$, as their coalescence is prevented by an increase in the anchoring energy $\sim W_p R_P^2$ and director-mediated repulsion [22].

For $R_p < L_p$, the anchoring effects are not essential, and E_V dominates in Eq. (1) to guide the particles toward the cites with the highest director gradients. Really, $\Delta E_S = (4\pi/15) W_p R_P^4 \,\mathrm{div}(\hat{\mathbf{n}}_0 \,\mathrm{div}\,\hat{\mathbf{n}}_0 + \hat{\mathbf{n}}_0 \times \mathrm{curl}\,\hat{\mathbf{n}}_0) \cong 4\pi W_p R_P^4 A^2/15\xi^2 \cong (2R_P/5L_P) E_V \ll E_V$ ($\hat{\mathbf{n}}_0$ is the director at the center of the LC volume replaced by the particle) and, according to [23], $|E_{ind}| \cong (W_p R_P/5A^2K)|\Delta E_S| \leqslant |\Delta E_S|$. The tendency of particles to occupy the regions with high elastic free energy prevails over the entropy driven randomization if $|\Delta E| \approx E_V \geqslant k_B T$ and, therefore, $R_P \geqslant R_C = \sqrt[3]{k_B T \xi^2/2KA^2}$. For $K = 10^{-11}$N, $\xi = 5\ \mu$m, $A = 1$, and room temperature, one finds $R_C = 0.2\ \mu$m. To estimate time τ, required to drive the particle, one can use the Stokes formula for the drag force $F \cong \Delta E/\xi \cong 6\pi\alpha_4 R_P \bar{v}$, where α_4 is the Leslie viscosity coefficient and $\bar{v} \cong \xi/\tau$ is the average velocity of the particle. Substitution $|\Delta E| \approx E_V$ in the Stokes formula results in $\tau \approx 9\alpha_4 \xi^4/KA^2 R_P^2$. For $\alpha_4 = 0.1$ Pa s, $\xi = 5\ \mu$m, $R_P = 1\ \mu$m, and $A = 1$, the driving time $\tau \sim 1$ min is small enough to provide accumulation of phase-separated particles. However, very smooth distortions (large ξ) may not be sufficient for the spatial inhomogeneity of a phase-separating component, as $\tau \propto \xi^4$.

Regular morphologies. Regular polymer architectures can be fabricated from regularly distorted director patterns, as we show below for "fingerprint" cholesteric textures in cells with homeotropic alignment (lecithin coatings). The cholesteric LC (pitch $p = 10\ \mu$m) was obtained by adding a chiral agent CB15 (EM Industries) to the E7/NOA65 mixture. The mixture was doped with a fluorescent dye acridine orange base (0.1 wt. %) for confocal polarizing microscope (Olympus Fluoview BX-50) observations. Confocal microscopy allows one to obtain micron-thin horizontal and vertical optical slices of the sample [4,9,11,24].

Before PS, the dye is distributed homogeneously [21], and the confocal polarizing microscope images the director field, as the dye is oriented by $\hat{\mathbf{n}}$ [24]. The vertical (xz) cross section of cholesteric texture has a diamondlike shape, with the axis tilted away from the z axis, Fig. 5(a). The corresponding computer-simulated equilibrium director $\hat{\mathbf{n}}(x,z)$ is shown in Fig. 5(b), and the local Frank-Oseen elastic energy density (calculated with different Frank constants [25]) in Fig. 5(c). The energy pattern shows that subsurface regions are distorted stronger than the bulk of the cell. It is easy to understand: in the bulk, $\hat{\mathbf{n}}$ has a favorable helical structure, whereas near the boundaries, perpendicular boundary conditions require energetically costly bend and splay.

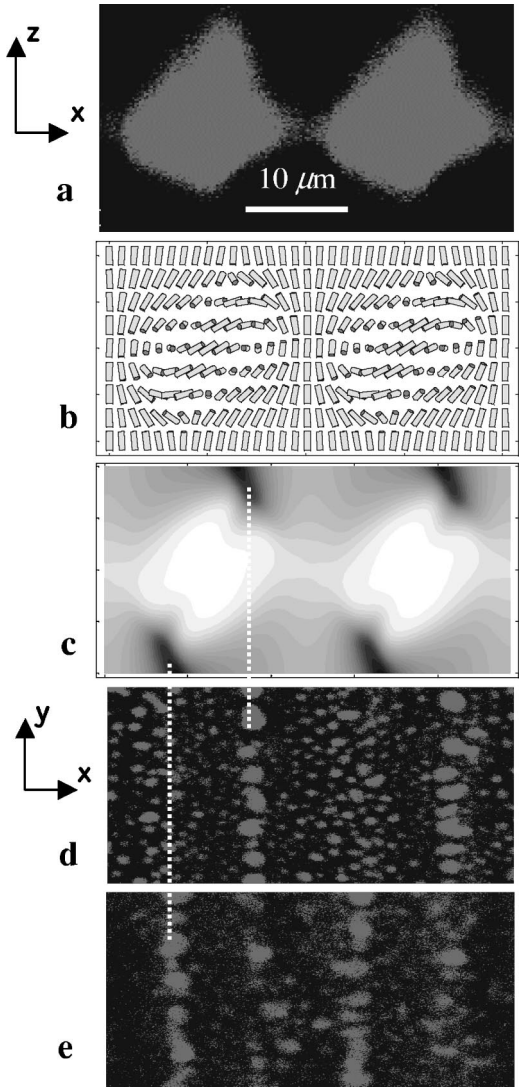

FIG. 5. Phase separation in a homeotropic cell ($d = 10\ \mu$m) with cholesteric "fingerprints." (a)–(c) are the vertical cross sections of the cell, and (d) and (e) are the horizontal ones. (a) Confocal texture of $\hat{\mathbf{n}}(x,z)$; (b) computer simulated $\hat{\mathbf{n}}(x,z)$ with Frank constants $K_1 = 6.4$, $K_2 = 3$, $K_3 = 10$ (all in pN), $W_c d/K = 10$; W_c is the anchoring coefficient at the plates; (c) map of the Frank-Oseen elastic energy density; higher energy densities are darker. Confocal textures of polymer particles near the upper plate (d) and the lower plate (e).

The PS morphology induced by nonpolarized UV-light is modulated in accordance with the fingerprint structure. In the phase-separated system, the acridine dye tends to accumulate in the polymer component rather than in the LC [26]. In the confocal textures, Figs. 5(d) and 5(e), the stained NOA65-rich particles appear bright on the dark LC background. A comparison of thin horizontal (x,y) optical slices reveals that the particles are located near the bounding plates exactly in the places with the maximum distortion energy, Figs. 5(c)–5(e) (the data are confirmed by scanning electron mi-

croscopy). Light polarization mechanism (a) also helps to accumulate NOA65 in these places, even when light is not polarized, as n_z component decreases in the diamond region.

We demonstrated that the director field can influence the PS patterns in an anisotropic solvent: the regions with the strongest distortions attract the phase-separating component. Further studies of PS morphologies in distorted LCs (role of the nature of components, properties of substrates, etc.) are of interest.

We thank L.-C. Chien, P. Palffy-Muhoray, S. Sprunt, J.L. West, and D.-K. Yang for useful discussions. The work was supported by the NSF ALCOM Grant No., DMR 89-20147 and by donors of the Petroleum Research Fund, administered by the ACS, Grant No. 35306-AC7.

[1] *Liquid Crystals in Complex Geometries*, edited by G. P. Crawford and S. Zumer (Taylor & Francis, London, 1996).
[2] I. Dierking, L.L. Kosbar, A. Afzali-Ardakani, A.C. Lowe, and G.A. Held, Appl. Phys. Lett. **71**, 2454 (1997).
[3] R.A.M. Hikmet and H. Kemperman, Nature (London) **392**, 476 (1998).
[4] K. Amundson, A. van Blaaderen, and P. Wiltzius, Phys. Rev. E **55**, 1646 (1997).
[5] T.J. Bunning, L.V. Natarajan, V.P. Tondiglia, and R.L. Sutherland, Annu. Rev. Mater. Sci. **30**, 83 (2000).
[6] Y. Kim, J. Francl, B. Taheri, and J.L. West, Appl. Phys. Lett. **72**, 2253 (1998).
[7] A.M. Lapena, S.C. Glotzer, S.A. Langer, and A.J. Liu, Phys. Rev. E **60**, 29 (1999).
[8] V. Vorflusev and S. Kumar, Science **283**, 1903 (1999).
[9] J.B. Nephew, T.C. Nihei, and S.A. Carter, Phys. Rev. Lett. **80**, 3276 (1998).
[10] J.-C. Loudet, P. Barois, and P. Poulin, Nature (London) **407**, 611 (2000).
[11] G.A. Held, L.L. Kosbar, I. Dierking, A.C. Lowe, G. Grinstein, V. Lee, and R.D. Miller, Phys. Rev. Lett. **79**, 3443 (1997).
[12] D. Voloschenko and O.D. Lavrentovich, J. Appl. Phys. **86**, 4843 (1999).
[13] S.W. Kang, S. Sprunt, and L.-C. Chien, Appl. Phys. Lett. **76**, 3516 (2000).
[14] J.A. Geurst, A.M.J. Spruijt, and C.J. Gerritsma, J. Phys. (France) **36**, 653 (1975).
[15] Technical Data Sheet for NOA65 Optical Adhesive, Norland Products, Inc., New Brunswick, NJ.
[16] G.W. Smith, Phys. Rev. Lett. **70**, 198 (1993).
[17] A.J. Lovinger, K.R. Amundson, and D.D. Davis, Chem. Mater. **6**, 1726 (1994).
[18] R. Bhargava, S.-Q. Wang, and J.L. Koenig, Macromolecules **32**, 2748 (1999); **32**, 8982 (1999); **32**, 8989 (1999).
[19] D. Nwabunma, K.J. Kim, Yu. Lin, L.-C. Chien, and Th. Kyu, Macromolecules **31**, 6806 (1998).
[20] L. Kielhorn and M. Muthukumar, J. Chem. Phys. **111**, 2259 (1999).
[21] Before PS, a concentration inhomogeneity could decrease the macroscopic elastic energy through concentration dependence of elastic constants. However, the entropy term strongly opposes such inhomogeneity, so the variation in concentration does not exceed 10^{-4} [S.V. Shiyanovskii and J.G. Terentieva, Phys. Rev. E **49**, 916 (1994)].
[22] P. Poulin, H. Stark, T.C. Lubensky, and D.A. Weitz, Science **275**, 1770 (1997).
[23] O.V. Kuksenok, R.W. Ruhwandl, S.V. Shiyanovskii, and E.M. Terentjev, Phys. Rev. E **54**, 5198 (1996).
[24] I.I. Smalyukh, S.V. Shiyanovskii, and O.D. Lavrentovich, Chem. Phys. Lett. **336**, 88 (2001).
[25] S.V. Shiyanovskii, I.I. Smalyukh, and O.D. Lavrentovich, in *Defects in Liquid Crystals, Computer Simulations, Theory and Experiments*, edited by O.D. Lavrentovich *et al.* (Kluwer, Amsterdam, 2001).
[26] S. Tahara, S. Niiyama, H. Kumai, and T. Wakabayashi, Proc. SPIE **3297**, 44 (1998).